JOURNAL OF Materials CHEMISTRY

Preparation and characterisation of tin-doped α-FeOOH (goethite)

Frank J. Berry,*[a] Örn Helgason,[b] Alberto Bohórquez,†[a] José F. Marco,[d] Julia McManus,[a] Elaine A. Moore,[a] Steen Mørup[c] and Paul G. Wynn[a]

[a]*Department of Chemistry, The Open University, Walton Hall, Milton Keynes, United Kingdom MK7 6AA*
[b]*Science Institute, University of Iceland, Dunhagi 3, Reykjavik, Iceland IS-107*
[c]*Department of Physics, Technical University of Denmark, Lyngby DK 2800, Denmark*
[d]*Instituto de Química Física 'Rocasolano', Consejo Superior de Investigaciones Científicas, c/Serrano 119, 28006 Madrid, Spain*

Received 8th February 2000, Accepted 25th April 2000
Published on the Web 9th June 2000

Tin-doped α-FeOOH (goethite) has been prepared directly by the hydrothermal processing of a precipitate. The morphology of the crystals, which is reflected in the ^{57}Fe Mössbauer spectra, depends on the pH of the precipitating media. The ^{119}Sn Mössbauer spectra are consistent with a complex microstructure around the octahedrally coordinated tin ions in the goethite structure and are sensitive to the changes in the magnetic structure of α-FeOOH resulting from tin doping. ^{57}Fe Mössbauer spectroscopy and electron microscopy show acicular tin-doped α-FeOOH to be converted to tin-doped α-Fe_2O_3 with identical morphology by mild heating in air.

Introduction

The iron oxyhydroxide of formula α-FeOOH, which is known as goethite, is widely found in natural environments. The structure is composed of double chains of iron in octahedral oxygen co-ordination which are further linked by sharing vertices in a three-dimensional framework structure. The preparation of the compound, together with aluminium-, manganese- and vanadium-substituted variants, has been described in detail.[1,2] Given that α-FeOOH is isostructural with α-AlOOH, α-MnOOH and VOOH it is not surprising that isomorphous replacement of some iron by trivalent ions such as aluminium, manganese and vanadium is possible. In contrast there appears to be a sparsity of data on α-FeOOH substituted by tetravalent ions.

We have recently reported[3,4] on our studies of the doping of α-Fe_2O_3 and γ-Fe_2O_3 by tetravalent tin. We have now extended this work to the doping of iron oxyhydroxides and we report here on the synthesis and characterisation of tin-doped α-FeOOH.

Experimental

Tin-doped α-FeOOH was prepared by precipitating aqueous mixtures of iron(III) nitrate (15.35 g, 100 ml) and tin(II) chloride (0.45 g, 10 ml) with aqueous ammonia at either pH 9.5 or 10.3 and hydrothermally processing the suspensions (*ca.* 260 ml) in a Teflon-lined autoclave at 200 °C and 15 atm pressure for 5 hours. The products were removed by filtration and washed with 95% ethanol until no chloride ions were detected by silver nitrate solution. The products were dried under an infrared lamp. The metal contents were determined by ICP analysis.

X-Ray powder diffraction patterns were recorded at 298 K with a Siemens D5000 diffractometer using Cu-Kα radiation.

The tin K-edge extended X-ray absorption fine structure (EXAFS) measurements were performed at the Synchrotron Radiation Source at the Daresbury Laboratory, UK, with an average current of 200 mA at 2 GeV. The data were collected in transmission geometry on Station 9.2 at 77 K. The raw data were background subtracted using the Daresbury program EXBACK and fitted using the non-linear least-squares minimisation program EXCURV92 which calculates the theoretical EXAFS function using fast curved wave theory.

Interatomic potential calculations were performed on a DEC alpha 600 workstation using the program GULP.[5] The optimised structure of goethite obtained by using literature potentials for oxygen and hydrogen in hydroxides[6] was far from satisfactory. All parameters for goethite were therefore obtained by fitting; the Buckingham potentials for Fe–O and O–O interactions were fitted using the standard fitting procedure in GULP, the Morse function was fitted by adjusting the parameters manually until a reasonable structure was obtained. Parameters for the Sn shell–O shell potential and the Sn spring constant were fitted using the O1–O1 potential obtained for goethite and fitting to tin dioxide. The calculated lattice parameters for goethite and tin oxide using our potentials are given in Table 1. The full set of potentials is given in Table 2. The oxygen atoms in the structure not bonded to hydrogen are indicated as O1 whilst O2 represents oxygen atoms forming OH groups. The radius of region 1 was taken to be 8 Å and region 2 was taken to be 16 Å.

X-Ray photoelectron spectra were recorded with a triple channeltron CLAM 2 analyser using Mg-Kα radiation and a constant analyser transmission energy of 100 eV for the wide scan spectra and 20 eV for the narrow scan spectra. Base pressure in the analyser chamber during the experiments was

Table 1 Lattice parameters for goethite and tin dioxide

	a/Å	*b*/Å	*c*/Å
Goethite experimental[9,10]	9.953	3.024	4.619
Goethite calculated	10.120	3.202	4.537
SnO_2 experimental[11]	4.737	4.737	3.186
SnO_2 calculated	4.539	4.539	3.325
Calculated lattice energies	L_0(FeOOH) = −76.81 eV		
	$L_0(SnO_2)$ = −115.45 eV		
	L_0(α-Fe_2O_3) = −147.13 eV		

†Permanent address: Departamento de Física, Universidad del Valle, AA25360, Cali, Columbia.

Table 2 Interatomic potentials

	Buckingham A/eV	Buckingham ρ/Å	C/eV Å^6	k/eV Å^{-2}	Core charge/e
Fe shell–O1 shell	1176.7687	0.33	0		
Fe shell–O2 shell	1109.9027	0.33	0		
O1 shell–O1 shell	19941974.999	0.149	27.88		
O2 shell–O2 shell	19941974.999	0.149	6.97		
O1 shell–O2 shell	7600005.623	0.149	13.94		
Sn shell–O shell	979.7289	0.3576	0		
Fe core–Fe shell				179.58	1.97
O1 core–O1 shell				74.92	0.86902
O2 core–O1 shell				74.92	0.86902
Sn core–Sn shell				191.5	0.01
H core					0.85

[a]Morse potential for O–H $D_e = 17.9937$ eV, $a = 3.86266$ Å^{-1}, $r_0 = 0.883$ Å.

ca. 2×10^{-8} Torr. All values of binding energy were charge converted to the C 1s signal (284.6 eV) and are accurate to ± 0.2 eV. Relative atomic concentrations were calculated using tabulated atomic sensitivity factors.[7]

The Mössbauer spectra were recorded between 17 and 298 K with a conventional constant acceleration spectrometer in transmission geometry. The ^{57}Fe Mössbauer spectra were recorded using a 400 MBq ^{57}Co/Rh source and the ^{119}Sn Mössbauer data were obtained with a 200 MBq $Ba^{119}SnO_3$ source. The drive velocity was calibrated with the ^{57}Co/Rh source and a natural iron foil. All the isomer shift data are reported relative to that of α-Fe at room temperature.

Electron micrographs were recorded from specimens suspended on copper grids using a JEOL 2000 FX electron microscope with an accelerating voltage of 200 KeV.

Results and discussion

The X-ray powder diffraction pattern recorded from the light brown powders (Fig. 1) shows the materials to be related to goethite, α-FeOOH. ICP analysis of the metal contents was consistent with a formulation α-$Fe_{0.86}Sn_{0.14}OOH$ in the material prepared at pH 9.5 and α-$Fe_{0.88}Sn_{0.12}OOH$ in that prepared at pH 10.3. The X-ray powder diffraction data were not amenable to refinement to a structural model. The tin K-edge EXAFS (Fig. 2, Table 3) were best fitted to a model in which tin was substituted for iron in the goethite structure.[8] Interatomic potential calculations for the substitution of Sn^{4+} ions on a Fe^{3+} site and for the insertion of Sn^{4+} ions into an interstitial site showed that there is a clear energy advantage for substitution over insertion into an interstitial site. The most favoured balancing defects of those considered were vacancies on the Fe^{3+} sites. The energies of the balanced defect reactions are given in Table 4. Reduction of Fe^{3+} to Fe^{2+} as a balancing reaction was not considered as the XPS results (*vide infra*) showed that Fe^{2+} is not present. Further support for

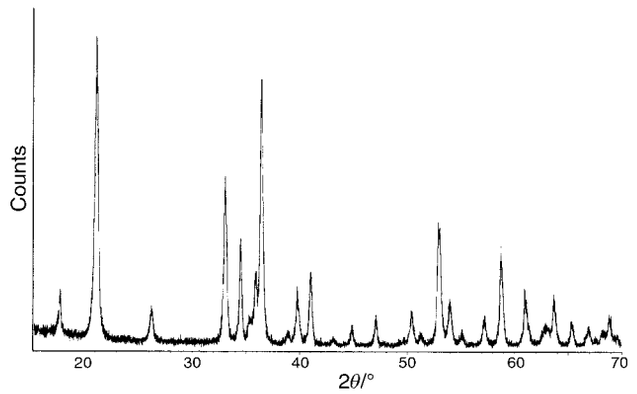

Fig. 1 X-Ray powder diffraction pattern recorded from tin-doped goethite.

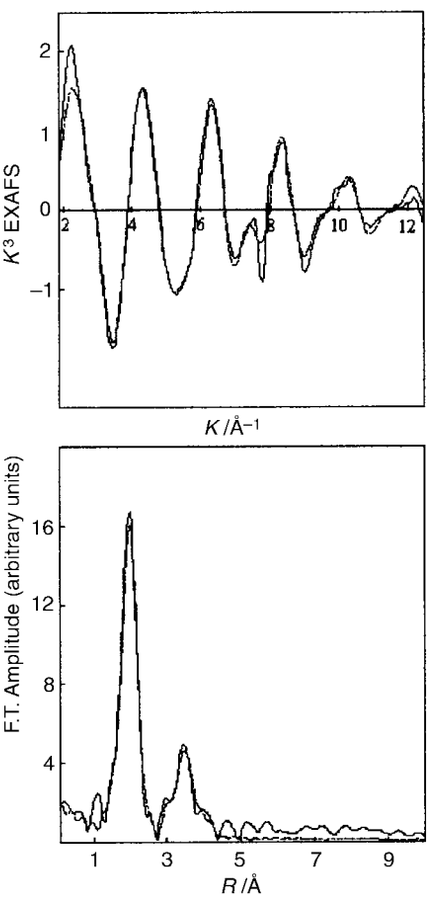

Fig. 2 Tin K-edge EXAFS and Fourier transform recorded from tin-doped goethite. The experimental data are indicated by the solid line.

substitution comes from the optimised structure around the Sn^{4+} ion. For Sn^{4+} substituted on an Fe^{3+} site, the optimised environment is similar to that of the Fe^{3+} ion in pure goethite,

Table 3 Best-fit parameters for tin K-edge EXAFS recorded from tin-doped goethite at 77 K

Atom type	Coordination number	Distance/Å $\pm 1\%$	$2\sigma^2$/Å^2
0	6	2.039	0.008
Fe	2	3.120	0.010
0	1	3.297	0.010
Fe	2	3.298	0.011
Fe	4	3.525	0.012
0	4	3.558	0.010
0	2	3.637	0.010
0	2	3.881	0.011
0	2	4.014	0.008

[a]$R = 15.80$.

Table 4 Energies of defect reactions in goethite

Balancing defect	Energy per Sn^{4+} ion/eV	
	Substitution of Sn^{4+} on Fe^{3+} site	Interstitial Sn^{4+}
Fe^{3+} vacancies	+2.85	+19.80
Fe^{3+} and O^{2-} vacancies	+12.13	+29.08
Fe^{3+} and OH^{-} vacancies	+11.04	+27.99

in agreement with the EXAFS data, but with Sn–O and Sn–Fe distances of the order of 0.2 and 0.06 Å greater than the original Fe–O and Fe–Fe distances. For the optimised interstitial Sn^{4+} ion there is one Sn–Fe distance of 2.8 Å, considerably shorter than the Fe–Fe distances in goethite.

The wide scan X-ray photoelectron spectra recorded from pure α-FeOOH and tin-doped α-FeOOH are shown in Fig. 3. Both spectra show the expected Fe 2p, Fe 3p, Fe (Auger), O 1s, C 1s, O (Auger) and C (Auger) contributions. The spectrum recorded from tin-doped goethite also shows a contribution from the Sn 3d level. The Fe/Sn atomic ratio calculated from the X-ray photoelectron spectra of *ca.* 7.5 is similar to that obtained by ICP analysis of the sample synthesised at pH 10.3. The result indicates that the surface concentration of iron and tin is similar to that found in the bulk of material. The Fe 2p and Fe 3p narrow scan spectra were also recorded from both samples. The peak corresponding to the Fe $2p_{3/2}$ core level of pure goethite at 711.3 eV was very similar to that reported[12] for pure goethite (711.4 eV), and the Fe 2p spectrum recorded from tin-doped goethite was identical except for the appearance of a shoulder at *ca.* 715.4 eV, which originates from the overlapping Sn $2p_{3/2}$ core level. The binding energy of the Fe 3p core level of pure goethite (55.3 eV) was identical to that recorded from tin-doped goethite (Fig. 4). Furthermore, the FWHM values of the Fe 3p peaks in the spectra recorded from pure α-FeOOH (3.3 eV) and tin-doped α-FeOOH (3.1 eV) were very similar. In our studies of tin-doped Fe_3O_4[13] we were able to detect the appearance of additional Fe^{2+} in Fe_3O_4 when doped with Sn^{4+} as a result of the charge balancing process. The X-ray photoelectron spectra recorded from tin-doped goethite showed no evidence for the formation of Fe^{2+} and demonstrate that charge balance is not achieved by the partial reduction of Fe^{3+} to Fe^{2+}. Given that ^{57}Fe Mössbauer spectroscopy also failed to show evidence for the reduction of Fe^{3+} to Fe^{2+} (*vide infra*) and the results of the interatomic potential calculations (*vide supra*) we envisage that charge balance in tin-doped goethite is achieved by the formation of cation vacancies.

Scanning electron microscopy showed the presence of needle-shaped particles up to *ca.* 400 nm in length in the sample precipitated from iron(III) nitrate and tin(II) chloride with aqueous ammonia at pH 10.3 (Fig. 5). The material

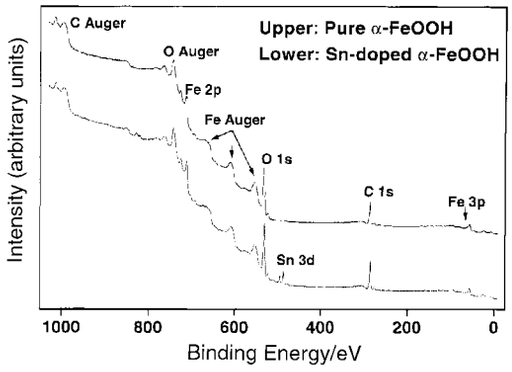

Fig. 3 Wide scan X-ray photoelectron spectra recorded from goethite and tin-doped goethite formed at pH 10.3.

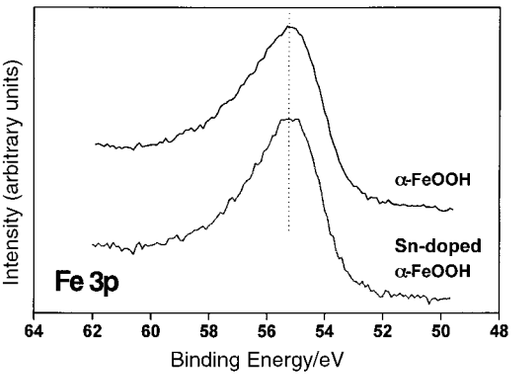

Fig. 4 Narrow scan Fe 3p X-ray photoelectron spectra recorded from goethite and tin-doped goethite formed at pH 10.3.

prepared at pH 9.5 was composed of rounded and smaller particles (*ca.* 25–50 nm) (Fig. 6).

The ^{57}Fe Mössbauer spectra recorded at 298 K from tin-doped goethite prepared at pH 9.5 and 10.3 (Fig. 7a) were similar to those previously recorded from natural goethite formed by the weathering of oxides, sulfides and silicates[14] and from pure synthetic goethite.[15–17] The origin of the line broadening in the Mössbauer spectra recorded from these types of materials has been the subject of much controversy.[15–18] The spectra were fitted to a model-independent distribution of the magnetic hyperfine fields.[19] All the linewidths of the sextets were kept fixed (0.23 mm s^{-1}) and the isomer shift and quadrupole splitting were kept constant in the final version of the fitting procedure (Table 5). The magnetic hyperfine field distributions (Fig. 7b) which characterise the samples prepared at pH 9.5 and 10.3 are different, and both the mean magnetic hyperfine field, $B_{\langle ave \rangle}$, and the hyperfine field at maximum probability, $B_{\langle max \rangle}$, are larger in the sample prepared at pH = 10.3. In both cases, the chemical isomer shift and quadrupole splitting data are similar and resemble those recorded from pure and aluminium-doped

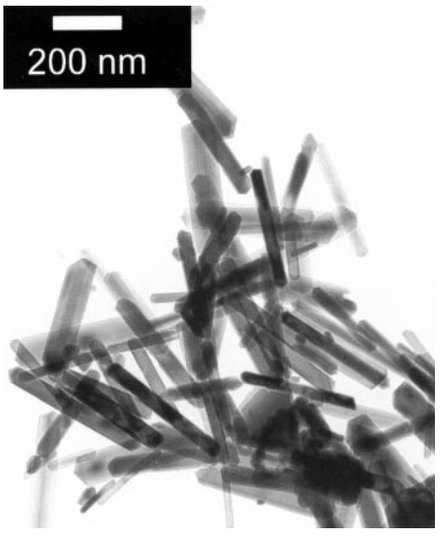

Fig. 5 Needle-shaped crystals of tin-doped goethite formed at pH 10.3.

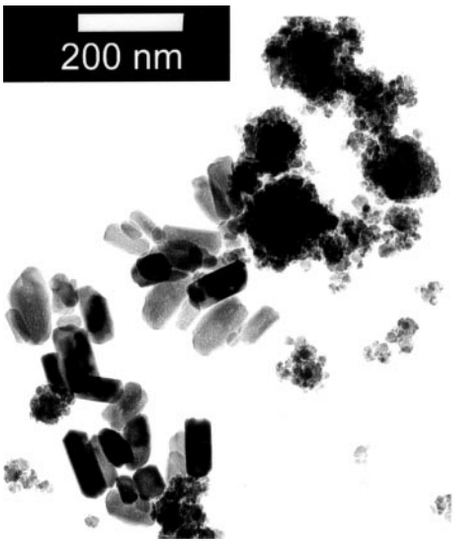

Fig. 6 Rounded crystals of tin-doped goethite formed at pH 9.5.

goethite.[15,16,20] The spectrum recorded from the sample prepared at pH 9.5 showed it to contain a small amount of α-Fe_2O_3 (less than 3% of total area); these data were excluded in all calculations relating to the results shown in Table 5. The differences between the spectra recorded from the samples prepared at pH 9.5 and 10.3 diminished as the temperature of measurement was decreased. Indeed, the spectra recorded from both samples at 80 K (Fig. 8) are very similar and can be fitted with nearly identical field distributions and hyperfine parameters (Table 5). The spectra recorded from both samples at 17 K were identical and show a smaller distribution in magnetic hyperfine fields, with a maximum value of 50.5 T. A spectrum at 17 K is shown in Fig. 8.

A comparison of the data recorded at 80 K from tin-doped α-FeOOH with those reported for aluminium-doped goethite[20,21] suggests that both tin and aluminium reduce the magnitude of the magnetic hyperfine field. In previous work,[20,21] the decrease in the magnetic hyperfine field was attributed to two different effects, the amount of dopant and the crystallinity, and empirical quantitative relationships were proposed. However, the earlier work on aluminium-doped goethite has been recently re-examined[22] and doubt has been cast on the proposed simple relationships between the amount of impurities, the crystallinity, and $B_{\langle max \rangle}$. In these circumstances it does not seem appropriate to make a quantitative comparison of the influence of tin and aluminium on the magnetic hyperfine field in goethite.

The ^{119}Sn Mössbauer spectra recorded at 298 K from tin-doped α-FeOOH formed at pH 9.5 and 10.3 are shown in Fig. 9a. The data were also fitted to a model independent distribution of magnetic hyperfine fields (Fig. 9b). Initial inspection suggests an absence of detailed structure and both spectra can be satisfactorily fitted to a broadened doublet with a wider linewidth than that characteristic of tin dioxide. However, the fitting of the data to a narrow doublet and a hyperfine magnetic field distribution with a maximum magnetic

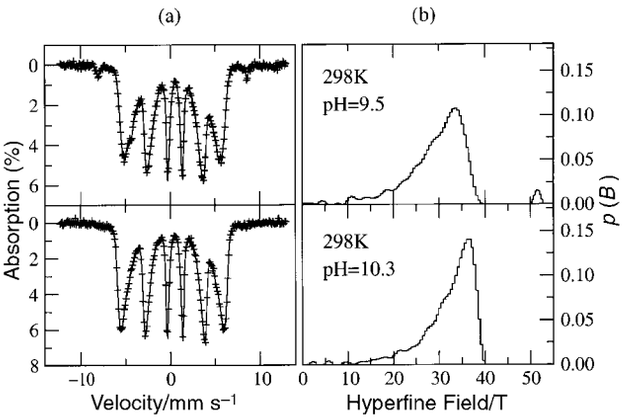

Fig. 7 (a) ^{57}Fe Mössbauer spectra recorded at 298 K from tin-doped goethite prepared at pH 9.5 and 10.3; (b) data fitted to a model independent distribution of magnetic hyperfine fields.

hyperfine field of 3–4 Tesla, reflecting the magnetic structure deduced by ^{57}Fe Mössbauer spectroscopy, is also appropriate (Fig. 9b). The room temperature data alone preclude unequivocal determination of the most superior fit. Support for the fit involving a magnetic interaction on the tin nucleus is obtained from the spectrum recorded at 17 K (Fig. 9a). In this spectrum a component with a larger magnetic hyperfine field can be resolved and the field distribution determined from the spectrum is shown in Fig. 9b. The ^{119}Sn Mössbauer hyperfine parameters are collated in Table 6. It appears that *ca.* 20% of the total tin content can be assigned to the spectral component with a maximum at 6.5 T and it might be reasonable to associate this with those tin ions which have only iron nearest cation neighbours. The other part of the magnetic hyperfine field distribution may reflect a more complicated environment

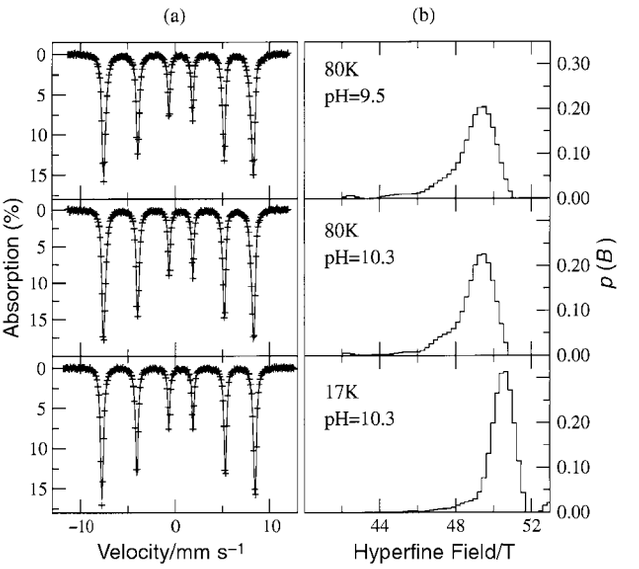

Fig. 8 (a) ^{57}Fe Mössbauer spectra recorded at 80 and 17 K from tin-doped goethite prepared at pH 9.5 and 10.3; (b) data fitted to a model independent distribution of magnetic hyperfine fields.

Table 5 ^{57}Fe Mössbauer parameters recorded from tin-doped goethite

T/K	pH of reaction mixture	$\delta(\pm 0.01)$/mm s^{-1}	$\Delta(\pm 0.01)$/mm s^{-1}	$B_{\langle max \rangle}$/T	$B_{\langle ave \rangle}$/T
298	9.5	0.37	−0.27	32.9	29.4
298	10.3	0.37	−0.28	36.2	31.6
80	9.5	0.47	−0.26	49.3	48.7
80	10.3	0.47	−0.26	49.6	49.0
17	10.3	0.48	−0.27	50.5	50.2

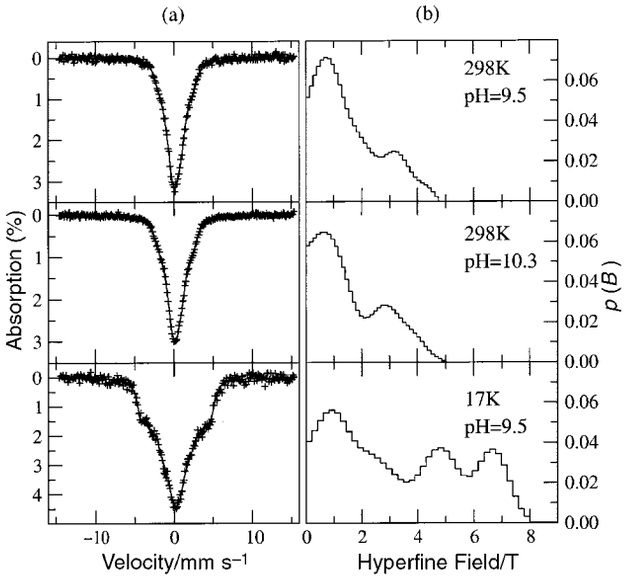

Fig. 9 (a) ^{119}Sn Mössbauer spectra recorded at 298 and 17 K from tin-doped goethite prepared at pH 9.5 and 10.3; (b) data fitted to a model independent distribution of magnetic hyperfine fields.

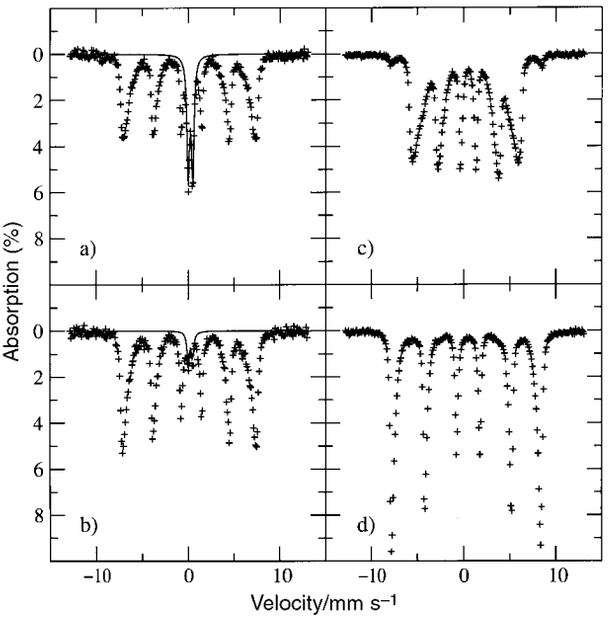

Fig. 10 ^{57}Fe Mössbauer spectra recorded for over 6 hours *in situ* from tin-doped goethite prepared at pH 10.3 following treatment at (a) 480 K (for 18 h), (b) 480 K (for 66 h), (c) room temperature before heating and (d) room temperature after heating.

about tin characterised by other factors such as vacancies or other tin ions. Taken together, the results suggest that dopant tin can be a sensitive means of probing the magnetic structure of goethite. The ^{57}Fe Mössbauer spectroscopy results at 298 K (Fig. 7, Table 5) indicate values of $B_{\langle max \rangle}$ of 33 and 36 T and $B_{\langle ave \rangle}$ of 29 and 32 T. At 17 K all these values are 50 T (Fig. 8). Assuming that the Sn^{4+} ions are distributed on the Fe^{3+} sites and that the magnetic hyperfine field sensed by Sn^{4+} is due to the antiferromagnetic structure of goethite, then the observation of similarly large increases in the magnitude of the magnetic hyperfine field in the ^{119}Sn Mössbauer spectra as the temperature decreases from 298 to 17 K (Fig. 9) is indicative of the sensitivity of tin to changes in the magnetic structure of goethite. The low field peak at about 1 T in the distribution of the spectrum recorded at 17 K exceeds the magnitude expected from an SnO_2 doublet (a value of Δ of 0.06 mm s^{-1} for the doublet equates to *ca* 0.4–0.5 T), although the calculation procedure cannot distinguish between a low field sextet and a paramagnetic doublet. This, together with the results from X-ray powder diffraction which showed no evidence for the presence of tin dioxide, supports the conclusion that tin has been incorporated within the goethite structure.

Finally, the sample produced at pH = 10.3 was heated to 480 K in a specially designed furnace[23] and examined *in situ* by ^{57}Fe Mössbauer spectroscopy. At 480 K the material showed a doublet characteristic of a paramagnetic material, as expected for a material *ca.* 100 K above the Néel temperature, but after less than one hour the spectrum showed the onset of a transformation to hematite, α-Fe_2O_3. After 24 hours at 480 K, 80% of the tin-doped goethite had transformed to α-Fe_2O_3 (Fig. 10a) and after 72 hours the doublet was hardly visible (Fig. 10b). The spectra recorded at room temperature before and after heating confirmed this transition (Fig. 10c and 10d) and, by comparison with earlier work on tin-doped hematite,[24] shows that the tin remains in the structure and has not segregated during the heat treatment. Separate heating of acicular tin-doped goethite at 370C (12 h) transformed the material to tin-doped α-Fe_2O_3 with similar morphology (Fig. 11).

Fig. 11 Acicular crystals of tin-doped α-Fe_2O_3 formed by heating tin-doped goethite at 370 °C (12 h).

Table 6 ^{119}Sn Mossbauer parameters recorded from tin-doped goethite

T/K	pH of reaction mixture	$\delta(\pm 0.01)$/mm s^{-1}	$\Delta(\pm 0.01)$/mm s^{-1}	$B_{\langle max \rangle}$/T	$B_{\langle ave \rangle}$/T
298	9.5	0.15	0.04	0.7 (3.1)[a]	1.5
298	10.3	0.16	0.04	0.7 (2.9)[a]	1.6
17	9.5	0.24	−0.03	0.8 (4.8 and 6.6)[a]	3.3

[a]Value for high field components in the distribution.

Acknowledgements

We thank the EPSRC for the award of a studentship (J. M.) and for beamtime at Daresbury Laboratory. We thank the Technical University of Denmark (O. H.) and also Colciencias and the Universidad del Valle (A. B.) for financial support. We acknowledge support from the European Union Socrates programme.

References

1 U. Schwertmann and R. M. Cornell, *Iron Oxides in the Laboratory*, VCH, Weinheim, 1991, p. 61
2 G. Brown, A. C. D. Newman, J. H. Raynor and A. H. Weir, in *The Chemistry of Soil Constituents*, ed. D. J. Greenland and M. H. B. Hayes, Wiley, Chichester, 1978, p. 135.
3 F. J. Berry, C. Greaves, J. G. McManus, M. Mortimer and G. Oates, *J. Solid State Chem.*, 1997, **130**, 272.
4 F. J. Berry, C. Greaves, Ö. Helgason and J. G. McManus, *J. Mater. Chem.*, 1999, **9**, 223.
5 J. D. Gale, *J. Chem. Soc., Faraday Trans.*, 1997, **93**, 629 [J. D. Gale, "General Utility Lattice Program (GULP)", The Royal Institution and Imperial College, London, 1992–1994].
6 P. S. Barum and S. C. Parker, *Philos. Mag. B*, 1996, **73**, 49.
7 C. D. Wagner, L. E. Davis, M. V. Zeller, J. A. Taylor, R. M. Richmond and L. H. Gale, *Surf. Interface Anal.*, 1981, **3**, 211.
8 A. Manceau and J. M. Combes, *Phys. Chem. Miner.*, 1988, **15**, 283.
9 A. Szytula, A. Burewic, Z. Dimitrievic, S. Krasnicki, H. Rzany, J. Todorovic, A. Wanic and W. Wolski, *Phys. Status Solidi*, 1968, **26**, 429.
10 J. L. Hazemann, J. F. Berar and A. Manceau, *Phys. Chem. Miner.*, 1992, **19**, 25.
11 R. W. G. Wyckoff, *Crystal Structures*, Wiley, New York, 1963, vol. 1, p. 251.
12 J. D. Walsh and P. M. A. Sherwood, *Phys. Rev. B*, 1989, **40**, 6386.
13 F. J. Berry, S. J. Skinner, Ö. Helgason, R. Bilsborrow and J. F. Marco, *Polyhedron*, 1998, **17**, 149.
14 A. Govaert, C. Dauwe, P. Plinke, E. De Grave and J. De Sitter, *J. Phys.*, 1976, **37**, C6–825.
15 S. Mørup, M. B. Madsen, J. Franck, J. Villadsen and C. J. W. Koch, *J. Magn. Magn. Mater.*, 1983, **40**, 163.
16 C. J. W. Koch, M. B. Madsen and S. Mørup, *Surf. Sci.*, 1985, **156**, 249.
17 S. Bocquet, R. J. Pollard and J. D. Cashion, *Phys. Rev. B*, 1992, **46**, 11 657.
18 J. M. D. Coey, A. Barry, J.-M. Brotto, H. Rakoto, W. N. Mussel, A. Collomb and D. Frucherd, *J. Phys. Condens. Matter*, 1995, **7**, 759.
19 C. Wivel and S. Mørup, *J. Phys. E*, 1981, **14**, 605.
20 E. Murad and J. H. Johnston, in *Mössbauer Spectroscopy Applied to Inorganic Chemistry*, ed. G. J. Long, Plenum, New York, 1987, vol. 2, p. 53.
21 C. A. Barrero, R. E. Vandenberghe, E. De Grave and G. M. da Costa, *Procedures of the International Conference on the Application of the Mössbauer Effect*, ed. I. Ortalli, S. I. F., Bologna, 1996, p. 717.
22 R. E. Vandenberghe, C. A. Barrero-Manese, G. M. de Costa, E. Van San and E. De Grave, *Hyperfine Interact.*, in press.
23 Ö. Helgason, H. P. Gunnlaugsson, K. Jónsson and S. Steinthorsson, *Hyperfine Interact.*, 1994, **91**, 595.
24 F. J. Berry, C. Greaves, Ö. Helgason, J. McManus and H. M. Palmer, *J. Solid State Chem.*, in press.